

## Article

# Organic Remains in Early Christian Egyptian Metal Vessels: Investigation with Fourier Transform Infrared Spectroscopy and Gas Chromatography–Mass Spectrometry

Kyriaki Koupadi <sup>1</sup>, Stamatis C. Boyatzis <sup>1,\*</sup> , Maria Roumpou <sup>2</sup> , Nick Kalogeropoulos <sup>2</sup>  and Despoina Kotzamani <sup>3</sup>

<sup>1</sup> Department of Conservation of Antiquities & Works of Art, University of West Attica, Aghiou Spyridonos, 12210 Egaleo, Greece; koupadikrk@gmail.com

<sup>2</sup> Department of Nutrition and Dietetics, Harokopio University of Athens, El. Venizelou 70, 17671 Athens, Greece; mroumpou@gmail.com (M.R.); nickal@hua.gr (N.K.)

<sup>3</sup> Metals, Glass and Organic Material Conservation Lab, Benaki Museum, Koubari 1, 10674 Athens, Greece; kotzamani@benaki.org

\* Correspondence: sboyatzis@uniwa.gr

**Abstract:** Organic remains preserved on eight copper alloy artifacts of the Byzantine Collection of the Benaki Museum with an Egyptian provenance were investigated, implementing a multi-analytical approach combining microscopy-FTIR and GC/MS. The transmission spectra of powder samples provided important information on the vessels regarding inorganic and organic components. In the latter case, subsequent extractions with a range of solvents allowed discrimination of components with different polarities and provided data on the suitability of the solvents for the acquisition of more informative spectra. GC/MS was implemented for the detailed characterization of the compounds present in the samples because of the complex nature of the residues preserved. A wide range of fatty acid oxidation products was identified, including a series of  $\alpha$ ,  $\omega$ -dicarboxylic acids typical of such remains. In addition, vicinal dihydroxy-docosanoic and dihydroxy-eicosanoic acid, oxidation products of erucic and gondoic acid, respectively, were detected. Both are found in abundance in oils from plants belonging to the Brassicaceae family and imply their multiple uses in medieval Egypt.

**Keywords:** organic archaeological remains; copper alloy; infrared spectroscopy; gas chromatography-mass spectrometry; solvent extraction; fatty acids; metal soaps



**Citation:** Koupadi, K.; Boyatzis, S.C.; Roumpou, M.; Kalogeropoulos, N.; Kotzamani, D. Organic Remains in Early Christian Egyptian Metal Vessels: Investigation with Fourier Transform Infrared Spectroscopy and Gas Chromatography–Mass Spectrometry. *Heritage* **2021**, *4*, 3611–3629. <https://doi.org/10.3390/heritage4040199>

Academic Editor: Nick Schiavon

Received: 31 August 2021

Accepted: 7 October 2021

Published: 18 October 2021

**Publisher's Note:** MDPI stays neutral with regard to jurisdictional claims in published maps and institutional affiliations.



**Copyright:** © 2021 by the authors. Licensee MDPI, Basel, Switzerland. This article is an open access article distributed under the terms and conditions of the Creative Commons Attribution (CC BY) license (<https://creativecommons.org/licenses/by/4.0/>).

## 1. Introduction

The application of analytical methodologies to archaeological material has revealed a range of organic molecules surviving over millennia. Organic remains have been identified in many archaeological contexts, and their study in the past 30 years has offered insights into plant and animal use and exploitation, trading of natural organic materials and their various uses [1,2]. Subsequently, archaeological research has focused on understanding the degradation pathways of the products utilized, during both use and deposition, and the identification of characteristic compounds that would allow the assignment of their origins [3–5]. Factors such as temperature, humidity, oxygen availability, and pH affect the preservation of different biomolecules [5–7].

The continuous development of new analytical methodologies has facilitated the characterization of a wide range of natural organic materials, such as animal fats and plant oils, beeswax, tars, and resins [1,8]. The identification of vegetable oils, known through literary sources to have been used in lighting, cooking, religious rituals, medications, and cosmetics, is particularly challenging, as they are very susceptible to degradation [9–13]. Partial hydrolysis of glycerol triesters occurs, gradually leading to mixtures of mono- and diacylglycerols, and eventually, free fatty acids and glycerol. Additionally, plant oils, rich in unsaturated moieties, undergo oxidative degradation mainly targeting double

bonds, involving mechanisms that lead to the formation of a wide array of oxidation products bearing hydroxyl, carbonyl, and carboxyl groups [14,15].

Gas chromatography–mass spectrometry (GC-MS) has provided important data and enabled molecular characterization of complex mixtures mainly in pottery vessels [10,16,17]. Ceramic containers are found in abundance in the archaeological record and therefore are a valuable source of information, ideal for residue analysis [2,18–21]. Organic residues in non-pottery vessels are not studied as frequently, although analysis of remains in metal and glass objects has presented promising results [22,23]. Visible residues adhering to metal candlesticks from the 12th century Fountains Abbey [24] were analyzed, along with residues found in a glass bottle from the Roman period recovered in Pompeii [25]. In the latter case, a multi-analytical approach using Fourier transform infrared (FTIR) spectroscopy was applied, which has been routinely used for the screening of complex samples, and it can also offer a more detailed characterization of archaeological samples [26–31]. In addition to transmission spectroscopy applied on powder samples, the development of reflection techniques, such as reflection–absorption (or transflection) in films on metal substrates, specular reflection, and attenuated total reflection (ATR) of surfaces, has assisted the investigation of coatings, consolidants, and adhesives [32–36]. Reflection–absorption FTIR [37–41] has been applied in the analysis of extracts [42] deposited as solution drops on reflective inert surfaces (such as gold); combined with microscopy, it may lead to detailed characterization of compounds or classes of compounds spatially separated from each other within a few micrometers and to the chemical mapping of surfaces [43,44]. Since infrared spectroscopy can be applied to samples without previous workup, the data obtained reflect their actual condition. Its combination with a powerful analytical technique such as gas chromatography–mass spectrometry provides robust information on organic samples.

In this work, a total of 16 objects from the Benaki Museum Byzantine Collection were initially screened through their transmittance spectra. This paper discusses in detail the results obtained using infrared spectroscopy and gas chromatography–mass spectrometry from eight objects (Figure 1), shown to contain organic components as mixtures of organic and inorganic materials. The objects are part of a larger collection comprising metal artifacts (128 metal vessels) of Egyptian provenance dated to the Late Antiquity (4th–8th Century A.D), which was acquired from street merchants in Cairo and is hence poorly documented. All objects were technologically and chemically investigated and conserved by the Benaki Museum (Metals, Glass, and Organic Material Conservation Laboratory) [45].

According to previous studies [45], these items were constructed of humble or “second class” materials, mainly a quaternary copper alloy (copper, zinc, tin, and lead) and were, therefore, characterized as utilitarian; another preliminary study also showed the existence of inorganic and organic remains in a large number of these objects [46]. In this study, questions regarding the nature of the visible remains preserved either in the interior of several lamps (lighting devices), small bowls (complimentary tableware items intended to contain a condiment), a spouted bowl (vessel carrying liquids for tableware, feeding lamp for babies, production of cosmetics), or around the attached areas between the parts of some pedestaled bowls (tableware or incense burners) [47] are systematically addressed. Also, information on the gap-filling material discovered in many artifacts during their conservation is presented. The investigation of plant oil uses in antiquity, and medieval Egypt in particular, builds upon the growing body of evidence derived from analytical techniques that aim at a better understanding of the everyday life activities of ancient societies. Furthermore, this work sheds light on residue analysis in largely overlooked container types, such as metallic artifacts, exploring the preservation of organic compounds in objects other than ceramics [22].



**Figure 1.** Photographs of the vessels selected for this work.

## 2. Experimental Procedures

### 2.1. Fourier Transform Infrared Spectroscopy

Fourier transform infrared spectra were recorded with a Perkin Elmer Spectrum GX 1 FTIR system. In the case of microscopy-FTIR, this was coupled with a PE AutoImage system. The recording conditions were as follows: for transmission spectra of KBr disks, 4000–400  $\text{cm}^{-1}$ , 32 or 64 scans and 4  $\text{cm}^{-1}$  resolution, DTGS detector at room temperature; for microscopy-FTIR spectra, 4000–700  $\text{cm}^{-1}$ , 100 scans, 100  $\times$  100 or 50  $\times$  50  $\mu\text{m}$  scanning areas, 4  $\text{cm}^{-1}$  resolution using a cryo-cooled (liquid  $\text{N}_2$ ) MCT detector

### 2.2. FTIR Analysis of Powder Samples in KBr Discs

According to a typical procedure, mid-infrared spectra of powder samples pressed in 13-mm KBr discs using a hydraulic press were recorded in transmission mode.

### 2.3. Solvent Extraction for FTIR Analysis

A solvent extraction scheme involving hexane, dichloromethane, acetone, and methanol was followed; solvents were selected according to their polarity and volatility. Approximately 5–10 mg of the powder sample was sonicated with 1 mL of solvent in a glass vial for 30 min. From each vial, one droplet of the supernatant fluid was accordingly deposited with a syringe on a neat KBr disc and left to dry at room temperature; complete solvent evaporation was monitored by FTIR. The remaining material was then analyzed in transmission mode. All spectra of solvent-extracted samples are shown not normalized so that relative intensities reflect the approximate relative quantities of extracted material; besides baseline correction, no other treatment was applied to spectra.

For microscopy-FTIR analysis, extraction in xylene and chloroform was conducted; droplets of solvent-extracted samples were accordingly deposited using a syringe on a 13 mm circular gold mirror plate and were left to dry at room temperature; complete solvent evaporation was monitored by FTIR. Consequently, the remaining material was

analyzed with a Perkin Elmer AutoImage microscopy-FTIR system in reflection mode, where different classes of compounds were analyzed on various spots deposited on the mirror disc. The working principle of this phenomenon lies in the spontaneous aggregation of chemically similar compounds in certain spots on the disc surface during solvent evaporation in a like-goes-with-like mode [48–50].

#### 2.4. Gas Chromatography–Mass Spectrometry

##### 2.4.1. Sample Preparation for GC-MS

The detached samples (quantities shown in Table S1, Supplementary Material) were labeled according to the object number and were extracted following standard extraction protocols (Charters et al. 1995; Stern et al. 2000). A solution of  $\text{CH}_2\text{Cl}_2:\text{CH}_3\text{OH}/2:1$  (2–4 mL) was added to the samples, that were then sonicated ( $2 \times 15$  min) and centrifuged (2000 rpm, 5 min). The excess solvent was transferred into a clean vial and evaporated under a gentle stream of nitrogen. A portion of the extract was saponified with  $\text{NaOH}/\text{CH}_3\text{OH}$  (0.5 M in a 70 °C, 60–90 min water bath). The resulting samples were acidified with 6 M HCl aqueous solution and extracted with  $3 \times 3$  mL of hexane. The supernatants were combined and transferred to glass vials and evaporated under a gently blown stream of nitrogen gas. All samples were subsequently converted to their trimethylsilyl derivatives using 80  $\mu\text{L}$  of *N,O*-bis(trimethylsilyl)-trifluoroacetamide (BSTFA, Sigma-Aldrich, St. Louis, MO, USA, derivatization grade >99.0%) [51–53].

##### 2.4.2. GC-MS Analysis

A Hewlett Packard series 6890 gas chromatograph equipped with a J&W GC fused silica capillary column, model DB-1HT (15 m, i.d.: 0.320 mm, film thickness 0.10  $\mu\text{m}$ , stationary phase composition: dimethylpolysiloxane) with helium as carrier gas and coupled to an Agilent Technologies series 7683 injector were employed. Samples were injected into the chromatograph in splitless mode; the oven temperature program was held isothermal at 50 °C for 2 min following injection; and ramped at a rate of 10 °C/s to reach 340 °C, which was kept for 14 min. The Mass Spectrometer (EI, 70 eV) was set to scan at 50–700 *m/z*. The TIC was recorded in all cases. For quantitation purposes 0.155 mg/mL of hexadecane/ $\text{CH}_2\text{Cl}_2$  solution as internal standard was used.

### 3. Results and Discussion

The nature of preserved residues found in a larger number of vessels has been addressed in previous studies. In these, analysis of inorganic remains [45] and preliminary screening of the residues [46] through transmission FTIR of powder samples (Table 1, column 2) were conducted. In light of this, further inquiries arose regarding the use, primary or secondary, of the residues in the vessels and lamps (for example, reused during later periods). Other hypotheses were based on the relationship of the contained materials to past repairs or post-excavation treatments. Moreover, the possible interactions of the most reactive substances among them with the existing metal ions because of the formation of corrosion products and/or other sources from the burial or atmospheric environment were also possible.

The sampled materials were investigated with infrared spectroscopy and gas chromatography–mass spectrometry. To this end, a systematic methodology was developed that correlates infrared spectra from powder samples, solvent-extracted residues, and standard GC-MS analysis. Key features in the mixture components within the samples were targeted, and possible links between the generated results were sought. Analytical results obtained through FTIR spectroscopy and GC-MS are summarized in Table 1.

**Table 1.** Infrared spectroscopy and gas chromatography–mass spectrometry results.

Sample Number; Description	KBr-FTIR Results	Organics through Solvent-Extracted FTIR Results	Organics through GC-MS
11544 Remain from interior	<i>Inorganics</i> <sup>a</sup> : Calcite (l.a.), silicates, SiO <sub>2</sub> (r); oxalates. <i>Organics</i> <sup>b</sup> : carboxylic acids, metal soaps (l.a.), esters.	<i>Methanol</i> : glyceryl mono- and diesters, fatty monoacids, diacids, and carboxylates (metal soaps). <i>Acetone</i> : acylglycerols (l.a.), saturated fatty monoacids (r.), anhydrides/lactones. <i>Dichloromethane</i> : acylglycerols, short/mid-chain fatty monoacids (r.)	FAs C16:0 (r.) and C18:0; diacids C9di and C13di; <i>Even-numbered sat.</i> FAs C8:0–C24:0; <i>Odd-numbered sat.</i> FAs: C9:0 and C15:0; <i>Unsat.</i> FAs: C16:1 and C18:1. Oxo- and hydroxy-FAs C6, C7, C8. Dihydroxy-FAs C18(diOH) and C22(diOH). Diacid series (C4di–C14di). C16- and C18-MAG (l.a.). Beta-sitosterol (l.a.). Glycerol (r.).
11550 Remain from interior	<i>Inorganics</i> <sup>a</sup> : Silicates, SiO <sub>2</sub> ; calcium oxalate (whewhellite), copper oxalate (moolooite) (r). <i>Organics</i> <sup>b</sup> : carboxylic acids, metal soaps, esters.	<i>Methanol</i> : glyceryl mono- and diesters, fatty monoacids, diacids, and carboxylates (metal soaps). <i>Acetone</i> : acylglycerols, fatty monoacids (r). <i>Dichloromethane</i> : acylglycerols (l.a.), short/mid-chain fatty monoacids (r.).	FAs: C16:0 (r.) and C18:0; diacids C8di, C9di (r.) and C13di. <i>Even-numbered sat.</i> FAs: C8:0–C26:0. <i>Odd-numbered sat.</i> FAs: C9:0 and C15:0. <i>Unsat.</i> FAs: C18:1. Full range of diacids: C4di–C14di. Glycerol (l.a.), MAG C16-G and C18-G; glyceric acid (tr).
11551 Remain from interior	<i>Inorganics</i> <sup>a</sup> : Silicates, SiO <sub>2</sub> , copper oxalate (moolooite). <i>Organics</i> <sup>b</sup> : carboxylic acids, metal soaps, esters.	<i>Methanol</i> : Glycerol and/or acylglycerols (r.), fatty acids (r.), diacids, carboxylates (metal soaps). <i>Acetone</i> : acylglycerols (r.), fatty monoacids (r.), diacids, anhydrides/lactones (l.a.). <i>Dichloromethane</i> : acylglycerols (r.), short/mid-chain fatty monoacids (r.).	C16:0 (r.), C18:0, C22:0 and C24:0 FAs; diacids C8di (r.), C9di and C13di. <i>Even-numbered sat.</i> FAs (l.a.): C8:0–C28:0 <i>Odd-numbered sat.</i> FA: C9:0 Glycerol (l.a.), C16- and C18-MAG; glyceric acid (tr). HCs: sat. C43–C49 and unsat. C28–C31. [meaning?]
11573 Remain from connection area	<i>Inorganics</i> <sup>a</sup> : calcite, silicates, calcium oxalate (whewhellite) (r). <i>Organics</i> <sup>b</sup> : carboxylic acids (l.a.), esters (l.a.).	<i>Methanol</i> : acylglycerols, carboxylates (metal soaps). <i>Acetone</i> : acylglycerols, fatty monoacids (r). <i>Dichloromethane</i> : acylglycerols, short/mid-chain fatty monoacids.	Diacids C8di, C9di (r.), C11di and C13di (r.). Glycerol (r.). <i>Even-numbered sat.</i> FAs C8:0–C24:0. <i>Odd-numbered sat.</i> FA: C9:0 MAG C16-G and C18-G. Diacids: C4di–C15di.
11596 Remain from interior	<i>Inorganics</i> <sup>a</sup> : calcium oxalate (whewhellite) (r). <i>Organics</i> : carboxylic acids (l.a.), esters (l.a.).	<i>Methanol</i> : Glycerol, carboxylates (metal soaps). <i>Acetone</i> : unspecified trace amounts. <i>Dichloromethane</i> : short/mid-chain fatty monoacids (l.a.).	Diacids C8di and C9di (r.). Glycerol and MAG C16-G and C18-G. <i>Even-numbered sat.</i> FAs C8:0–C24:0. <i>Odd-numbered sat.</i> FA: C9:0 MAG C16-G and C18-G. Diacids: C4di–C14di. HCs: sat. C23, C24, C27, C30.
11598 Remain from interior	<i>Inorganics</i> <sup>a</sup> : calcite (l.a.), silicates (r), oxalates. <i>Organics</i> <sup>b</sup> : carboxylic acids, carboxylate salts (tr), esters.	<i>Methanol</i> : acylglycerols, fatty acids, carboxylates (metal soaps). <i>Acetone</i> : acylglycerols. <i>Dichloromethane</i> : short/mid-chain acylglycerols (r.), fatty monoacids (tr.).	Diacids C8di and C9di (r.). Glycerol and MAG C16-G and C18-G. <i>Even-numbered sat.</i> FAs C8:0–C24:0. <i>Odd-numbered sat.</i> FA: C9:0 and C17:0 <i>unsat.</i> FAs: C18:1. MAG C16-G and C18-G. Diacids: C4di–C14di. HCs: sat. C23, C24, C27, C30. Hypoxanthine, maltose (possible contaminants).

Table 1. Cont.

Sample Number; Description	KBr-FTIR Results	Organics through Solvent-Extracted FTIR Results	Organics through GC-MS
11622A Remain from cavities in connection area	<i>Inorganics</i> <sup>a</sup> : silicates (l.a.), calcium oxalate (whewhellite) (r.) <i>Organics</i> <sup>b</sup> : carboxylic acids (l.a.), carboxylate salts (tr.), esters.	<i>Methanol</i> : acylglycerols, carboxylates (metal soaps). <i>Acetone</i> : acylglycerols. <i>Dichloromethane</i> : acylglycerols, short/mid-chain fatty monoacids.	Dihydroxy FA: 13,14-dihydroxy C22:0 FA (r.); Diacids C8di, C9di (r.) and C11di (r.); Glycerol (r.). Even-numbered sat. FAs C8:0–C24:0. Odd-numbered sat. FA: C9:0 MAG: C16-G and C18-G Diacids: C4di–C15di. Dehydroabiatic acid and 7-oxo-dehydroabiatic acid.
11622B Powder from addition on vessel body	<i>Inorganics</i> <sup>a</sup> : Gypsum (r.), calcite, silicates, SiO <sub>2</sub> (r). <i>Organics</i> <sup>b</sup> : n.d.	No organics found.	n.a.
11633A Remain from connection area	<i>Inorganics</i> <sup>a</sup> : Silicates, SiO <sub>2</sub> , (r), calcium oxalate (whewhellite) (r), copper oxalate (moolooite) (tr.). <i>Organics</i> <sup>b</sup> : carboxylic acids (l.a.), metal soaps (r.), esters (l.a.).	<i>Methanol</i> : acylglycerols, carboxylates (metal soaps). <i>Acetone</i> : acylglycerols. <i>Dichloromethane</i> : acylglycerols, short/mid-chain fatty monoacids (r.).	Glycerol (r.); C22(diOH) (r). Even-numbered sat. FAs C8:0–C24:0. Odd-numbered sat. FA: C9:0 and C17:0. MAG: C16-G and C18-G. Diacids: C4di–C15di.
11633B Powder from interior remains	<i>Inorganics</i> <sup>a</sup> : Gypsum (r.), calcite, silicates, SiO <sub>2</sub> . <i>Organics</i> : n.d.	No organics found.	n.a.

<sup>a</sup>: assignments from [46]. <sup>b</sup>: assignments based on [46], enriched in the light of this work. n.d.: not detected; n.a.: not applied; r.: rich; tr.: traces, l.a.: low amounts; G: glycerol.

### 3.1. Fourier Transform Infrared Spectroscopy

#### 3.1.1. Powder Samples

Transmission spectra of all samples are shown in Figure 2, while peak assignments are listed in Table 2. Powder samples detached from the interior of objects (samples #11544, 11550, 11551, 11596, 11598, 11633B) and cavities in the connection areas of objects (samples #11573, 11622A, 11622B, and 11633A) were analyzed with KBr-FTIR. Significant quantities of silicates (with characteristic infrared peaks at 1030, 517, 465  $\text{cm}^{-1}$ ) and/or quartz sand (1090  $\text{cm}^{-1}$ , and the 790/779  $\text{cm}^{-1}$  doublet) were found in most objects, except the small bowl (#11596) and pedestaled bowl (#11622A). Calcium oxalate, possibly the biogenically formed whewellite (maxima at 1623, 1317, and 780  $\text{cm}^{-1}$ ) [54], was detected in most objects; high quantities were found particularly in the small bowls (#11596 and 11573) and the two pedestaled bowls (#11622 and 11633). In addition, small amounts of copper oxalate (or moolooite), with maxima at 1618, 1360, and 817  $\text{cm}^{-1}$  were detected in oil lamps #11550 and 11551 [55]. Most possibly, oxalates were the reaction product of biogenic oxalic acid with calcium salts and copper corrosion materials [55,56].

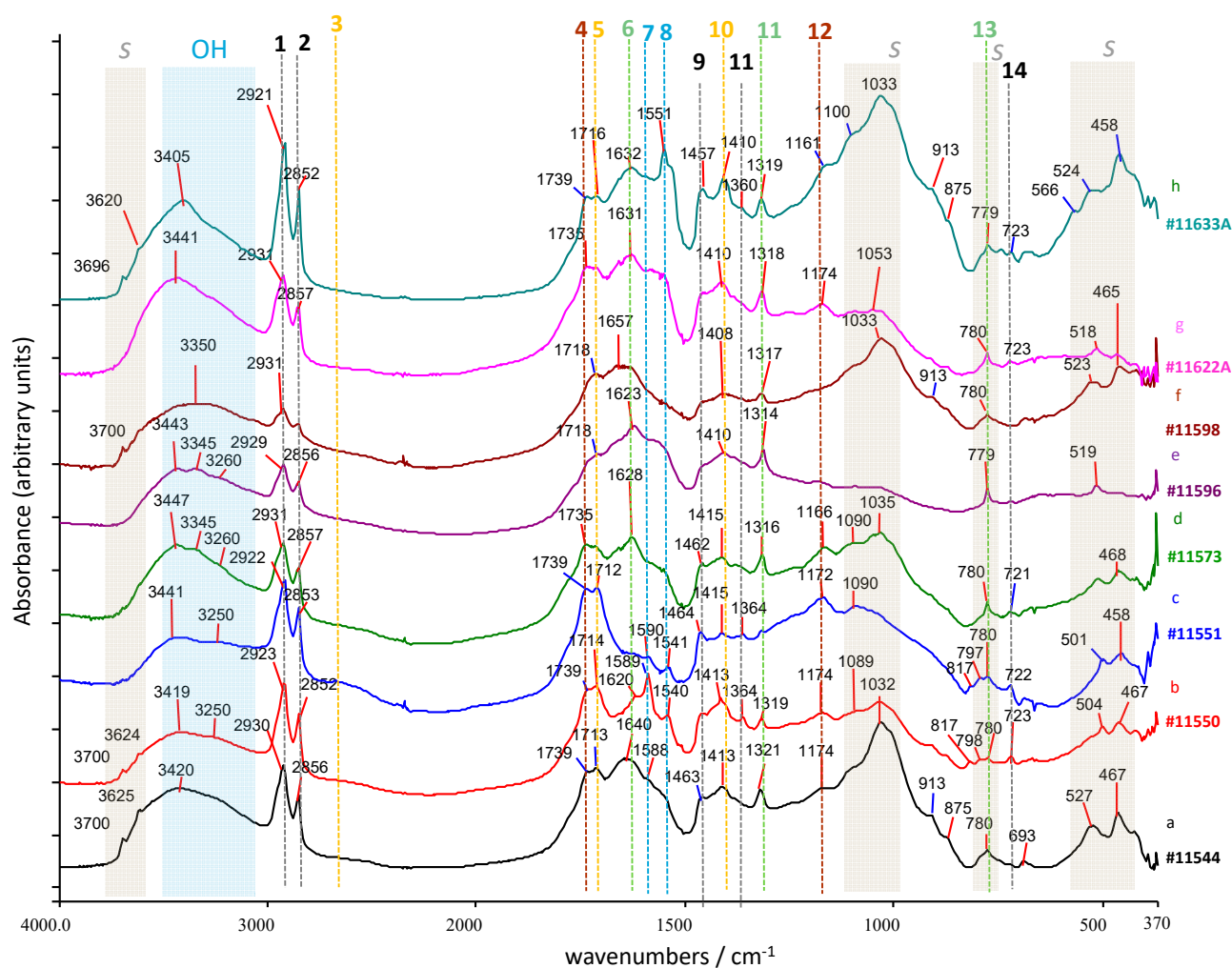


**Figure 2.** KBr-FTIR spectra of powder samples from the selected vessels. Shaded areas: S = silicates and quartz sand; OH = hydroxyl groups in organics (free FA, acylglycerols). Vertical lines: 1, 2, 9, 11, 14 = alkyl chain vibrations; 3, 5, 10 = free FA; 4, 11 = FAE; 6, 11, 13 = oxalates; and 7, 8 = metal carboxylates. All spectra shown after baseline correction with no further workup.

**Table 2.** Assignments of main infrared peaks detected in investigated samples.

Maximum, Wavenumber (cm <sup>-1</sup> )	Assignment <sup>1</sup>	Type(s) of Compounds
3700–3696	$\nu$ OH	Hydroxides or crystalline water in silicates (clay)
3624–3620	$\nu$ OH	Hydroxides or crystalline water in silicates (clay)
3440–3400 (br)	$\nu$ OH	Hydroxyl in acylglycerols, hydroxy-acids Adsorbed water in silicates
3300–3200	$\nu$ OH	Carboxyl in free FA
2960–2950	$\nu_{as}$ CH <sub>3</sub>	FA and FAE
2951–2937		Diacids
2940–2935		C4–C6
2930–2920	$\nu_{as}$ CH <sub>2</sub>	C7–C12
2918–2910		C13–C18
1740–1730		Fatty esters (acylglycerols)
1718–1712		Short-chain fatty monoacids (C4–C9)
1711–1709	$\nu$ C=O	Mid-chain fatty monoacids (C10–C12)
1708–1701		Long-chain fatty monoacids (>C12)
1700–1695		Diacids
1650–1630 (br)	$\delta$ OH	Adsorbed water in silicates
1640	$\nu_{as}$ COO <sup>-</sup>	Copper oxalate (moolooite)
1623	$\nu_{as}$ COO <sup>-</sup>	Calcium oxalate (whewhellite)
1590		
1551	$\nu_{as}$ COO <sup>-</sup>	Fatty acid metal salts
1541		
1470	$\delta$ CH <sub>2</sub>	Alkyl chains in diacids and fatty esters (acylglycerols)
1458	$\delta$ CH <sub>2</sub>	Alkyl chains in monocarboxylic acids
1425	$\delta_{ip}$ C–O–H	Diacids
1412	$\delta$ CH <sub>2</sub>	Alkyl chains in diacids
1414–1408	$\delta_{ip}$ C–O–H	Fatty monoacids
1393	$\delta_{ip}$ C–O–H	Alcohol in glycerol or glyceryl group
1380–1364	$\delta_s$ CH <sub>3</sub>	Terminal methyl groups in fatty monoacids and their glycerol esters; relatively stronger as compared to $\delta$ CH <sub>2</sub> in short-chain monoacids
1317	$\nu_s$ COO <sup>-</sup>	Calcium oxalate (whewhellite)
1180	$\nu$ C–O–C=O	Copper oxalate (moolooite)
1105	$\nu$ C–O–C=O	Ester links (acylglycerols)
1090	$\nu$ Si–O	Ester links (acylglycerols)
	$\nu$ Si–O	Silicates: quartz sand
1026	$\nu$ C–O–H	Silicates: clay
817	$\delta$ OCO	Glycerol or glyceryl group
780	$\delta$ OCO	In carboxylates: copper oxalate (moolooite)
798/779	$\nu_{as}$ Si–O–Si	In carboxylates: calcium oxalate (whewhellite)
722, 691	$\rho$ CH <sub>2</sub>	Silicates: quartz sand
527	$\delta$ OSiO	Long alkyl chain of fatty acids and salts
467	$\delta$ OSiO	Silicates
		Silicates

<sup>1</sup>  $\nu$  = stretching,  $\nu_{as}$  = anti-symmetric stretching,  $\nu_s$  = symmetric stretching,  $\delta_{as}$  = anti-symmetric bending,  $\delta_s$  = symmetric bending (umbrella type),  $\delta_{i-p}$  = in-plane bending,  $\delta_{o.o.p}$  = out-of-plane bending vibration,  $\rho$  = rocking vibration, br = broad. Bold letters signify the bond vibrations in focus.

In addition to the above, a generally rich organic fraction was detected based on the prominent alkyl chain peaks at 2922, 2853 (various C-H stretching vibrations), 1464, 1415 ( $\delta$ CH<sub>2</sub>), 1364 cm<sup>-1</sup> ( $\delta_s$ CH<sub>3</sub>) and, in few cases, 724 cm<sup>-1</sup> (CH<sub>2</sub> rocking) [57–60]. Moreover, the carbonyl stretching bands at ~1735 cm<sup>-1</sup> (ester carbonyl), ~1713 cm<sup>-1</sup> (acidic carbonyl), and 1600–1540 cm<sup>-1</sup> (antisymmetric carboxylate stretch) provided evidence for fatty acid esters in lipids, free fatty acids (FAs) and their metal salts (FAMS), respectively, in most samples. Finally, the broad hydroxyl stretching band at 3500–3100 cm<sup>-1</sup> was detected in all samples assignable to alcoholic hydroxyl groups, presumably, glycerol and its mono- and diesters. The above assignments were supported by the additional detection of (a)

$\nu$ O-H at  $2657\text{ cm}^{-1}$  for the dimeric acids, more prominent in samples #11544, 11550, 11551, and 11573, and (b)  $1240$ ,  $1171$ , and  $1093\text{ cm}^{-1}$  for C-O ester links (intense in most samples, weak in #11596, 11598).

Furthermore, carboxylate bands at  $1587$  and  $1541\text{ cm}^{-1}$  (antisymmetric  $\text{COO}^-$  stretch [61]), more prominent in samples #11633A, 11550, and 11551, were detected, assignable to salts and complexes of fatty acids with metals [62,63]. In light of detecting free fatty acids through SE-FTIR and GC-MS analysis (see below), the soaps may have been formed through the interaction between the free fatty acids and metal ions, arguably copper or calcium [62]. Between the two, copper appeared more plausible as it was the main metal in the body of all vessels, while very low amounts of calcium carbonate (the main geogenic calcium source [54]) were detected in the transmission spectra. The formation of metal soaps is chemically favored in the archaeological environment since they are relatively insoluble in water and, being more stable, they contribute to better preserving the lipid character in time [63].

The detection of metal soaps raised the question of possible contamination of the contained material through cleaning actions at an unspecified time. However, sodium fatty acid salts could be ruled out since elemental analysis did not detect sodium. Further supporting this hypothesis, no sodium carboxylate peaks (expected at  $1560$  and  $1423\text{ cm}^{-1}$  for their antisymmetric and symmetric stretching vibrations, respectively [64–67]) were detected by FTIR.

Instead, calcium and copper soaps were most possibly detected as deterioration products of fatty acids in the presence of certain metal ions such as lead, zinc, copper, and calcium [66,68–70]; besides, the relatively narrow line shapes of most bands suggested well-crystallized soaps [71]. This fact added an originality asset to the organic remains profile of the objects in this study.

Most of the above transmission spectra results were better evaluated in the light of solvent-extraction infrared spectroscopy (SE-FTIR) and GC-MS results.

### 3.1.2. Solvent-Extracted FTIR Results

An analytical scheme focusing on the organic fraction was implemented to overcome interpretation uncertainties in KBr infrared spectra of powder samples from peak overlaps between organic and inorganic components. Previous works have reported solvent extractions for acquiring infrared spectra of isolated components [42,72,73]. Here, a coordinated solvent extraction scheme based on polarity, involving methanol, acetone, and dichloromethane, while in microscopy-FTIR, chloroform and toluene, were considered. Infrared spectra were recorded from the dried remain on KBr discs after dripping solvent extracts of samples; this technique will be referred to as solvent-extracted FTIR (SE-FTIR, see Materials and Methods), with results for all samples shown in the Supplementary Information file, Figures S1–S4.

Methanol extracts: Methanol extracts corresponded to the relatively polar fraction of the entire component range, as comparatively shown in Figure S1. Extracts were found to be rich for samples #11550 (Figure 3b), #11551 (Figure 4b), #11596, 11598, and 11633, where ester carbonyl (observed at  $1737$ – $1729\text{ cm}^{-1}$ ) and hydroxyl groups (broad maxima at  $3400$ – $3300\text{ cm}^{-1}$ ), were detected and attributed to glyceryl esters, mainly mono- and diesters (MAG or DAG). The C-O stretch at  $1020$ – $1025\text{ cm}^{-1}$ , and  $1110$ – $1130\text{ cm}^{-1}$  ( $\text{C}^1$ -OH and  $\text{C}^2$ -OH, respectively), in addition to their ester C-O ester links ( $1180\text{ cm}^{-1}$ ), with the broad maxima at  $\sim 3400\text{ cm}^{-1}$  supported the mono- and di-acylglycerol assignment [74–76].

The  $\text{CH}_2$  antisymmetric maxima were upshifted to  $2930$ – $2925\text{ cm}^{-1}$  for medium- and short-chain (<C10) fatty acids, detected in samples #11573, 11596, 11598, 11622A; the acidic carbonyl maxima at ca.  $1717$ – $1713\text{ cm}^{-1}$  supported this assignment [28,31,64,74,77–79]. Finally, shoulders at  $\sim 1700\text{ cm}^{-1}$  in samples #11550 and 11551 suggested the presence of diacids [64], which were confirmed through the GC-MS results (see below).

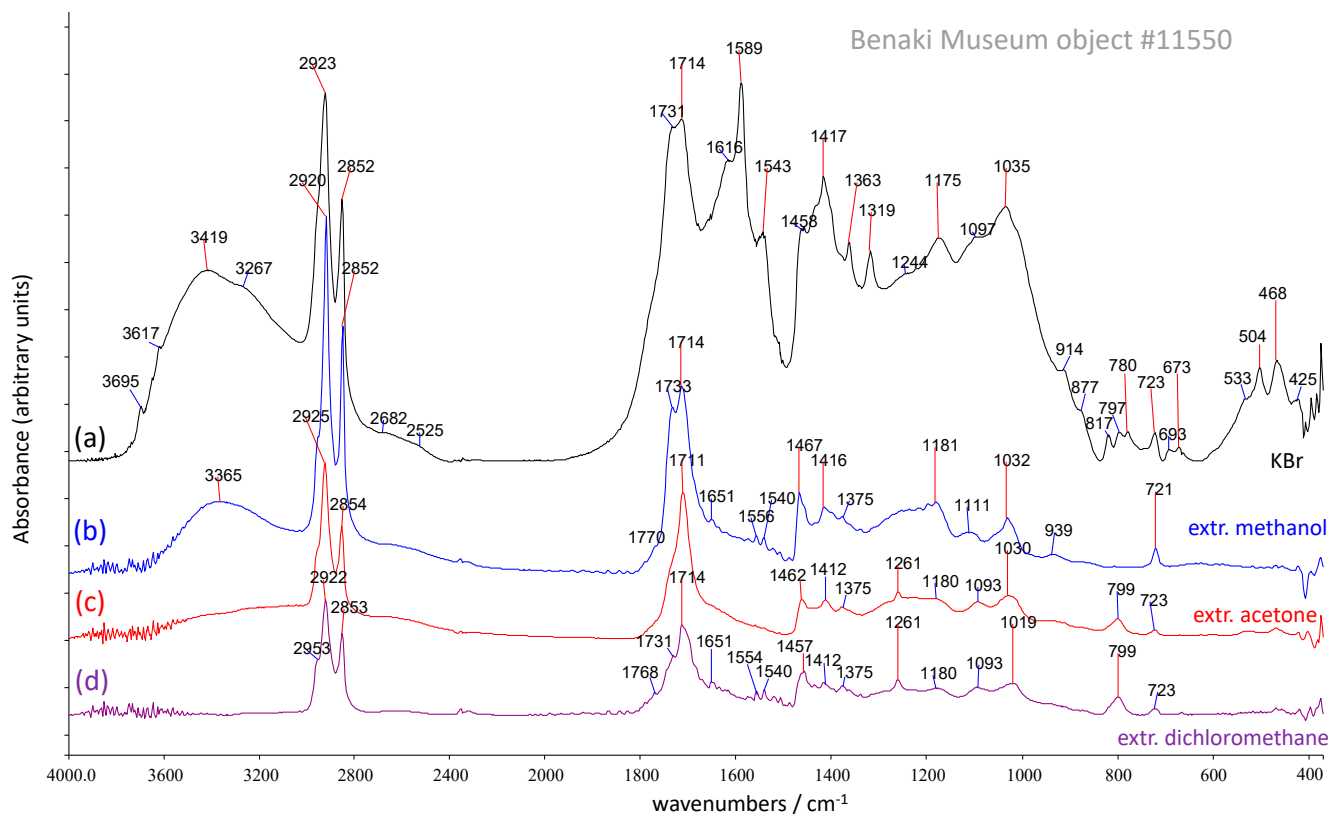


**Figure 3.** Infrared spectra of sample #11550; (a) powder sample (KBr); (b) methanol–extracted; (c) acetone–extracted; and (d) dichloromethane–extracted components.

In the light of GC-MS analysis, where a significant fraction of dicarboxylic acids was identified (see below), evidence for dicarboxylic fatty acids (di-FAs), typical degradation products of unsaturated oils, was provided in the infrared spectra of methanol extracts #11544 and 11550. This was based on the absence of the  $\text{CH}_3$  vibrations, the low-shifted carbonyl maxima (shoulder at  $\sim 1700\text{ cm}^{-1}$ ), their relatively high-shifted antisymmetric  $\text{CH}_2$  stretch (shoulder at  $2960\text{--}2950\text{ cm}^{-1}$ ), and their in-plane  $\text{CH}_2$  and C-O-H bending (diagnostically appearing at  $\sim 1425$  and  $\sim 1412\text{ cm}^{-1}$ , respectively) [64].

Finally, fatty acid metal salts (FAMS) through a shoulder at  $1560\text{--}1550\text{ cm}^{-1}$  were also detected in samples #11551, 11550, 11633A, 11622A, 11573, and 11596. Compared to transmission spectra of powdered samples (see above), soaps were detected in significantly lower amounts in SE-FTIR spectra because of their limited solubility in the used solvents.

Acetone extracts: As seen through their SE-FTIR spectra, acetone extracts were particularly rich in detected components, comparatively shown in Figure S2. Esters were almost exclusively present in most samples (#11573, 11596, 11598, 11622, 11633) based on their carbonyl absorption at  $1745\text{--}1730\text{ cm}^{-1}$  and confirmed by their methylene and methyl stretching ( $\sim 2920$ , and  $2955\text{ cm}^{-1}$ , respectively) and bending vibrations ( $\sim 1470$  and  $1460/1380\text{ cm}^{-1}$ , respectively) [74,80]. In addition, evidence of fatty anhydrides or lactones was also visible (shoulders at  $1780\text{--}1765\text{ cm}^{-1}$  [81]) as products of intense oxidation [28,82]. Spectra for samples #11550 and 11551 are shown in Figure 3c or Figure 4c, compared to corresponding spectra from other solvents.

On the other hand, FAs with medium alkyl chains were detected in the oil lamp samples (#11544, 11550, and 11551) on the basis of their acidic carbonyl absorptions ( $1710\text{--}1700\text{ cm}^{-1}$ ), supported by their methylene stretching ( $\sim 2925\text{ cm}^{-1}$ ), bending ( $\sim 1460\text{ cm}^{-1}$ ), and rocking maxima ( $\sim 720\text{ cm}^{-1}$ ) [57,58,60,83]. Esters were also detected in the same samples but in lower amounts.

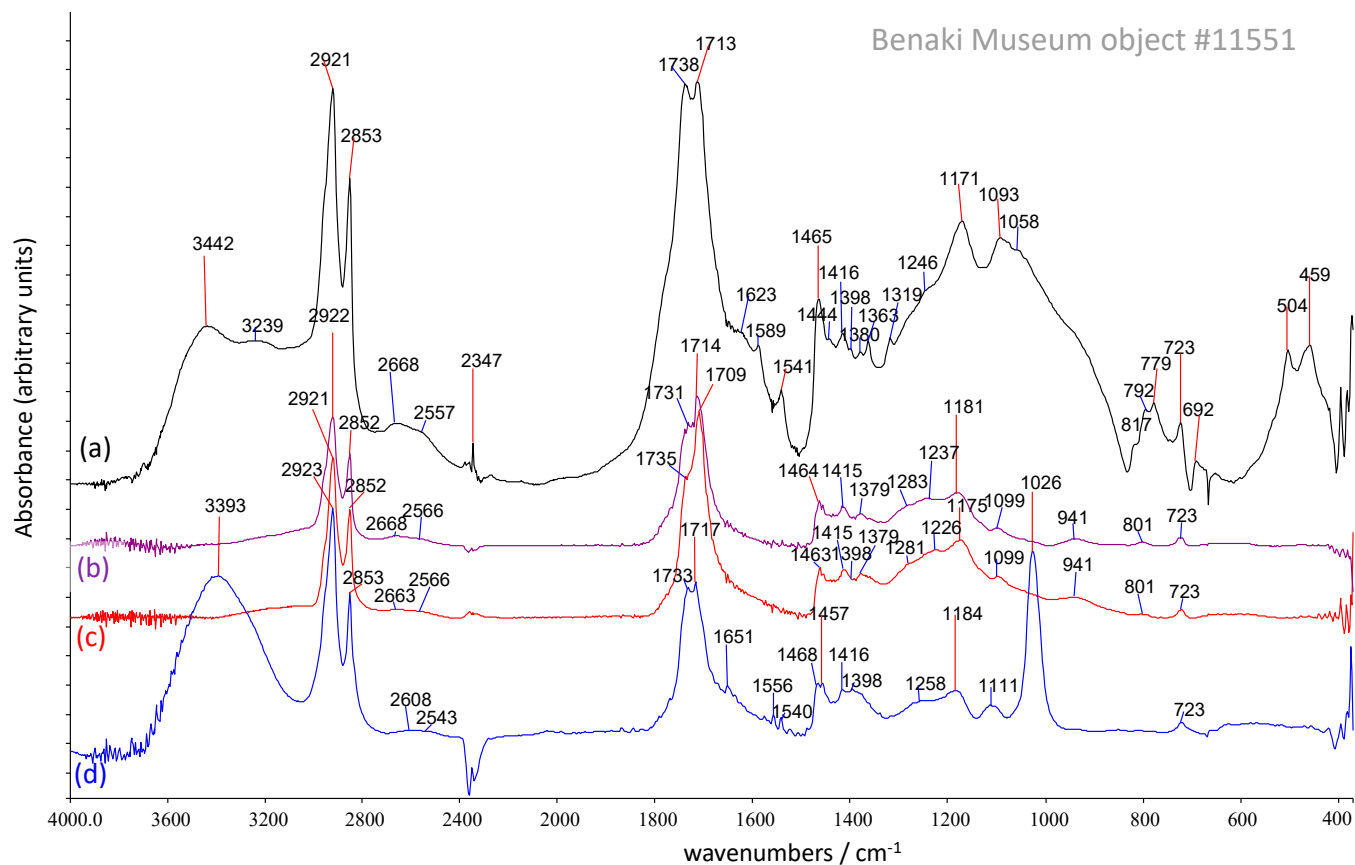


**Figure 4.** Infrared spectra of sample #11551; (a) powder sample (KBr); (b) dichloromethane-extracted; (c) acetone-extracted, and (d) methanol-extracted components.

Dichloromethane extracts: Extraction with dichloromethane resulted in rich SE-FTIR spectra (Figure S3). A general characteristic of most spectra was the prominence of methyl groups' absorptions (i.e., stretching at  $2958 \text{ cm}^{-1}$  and bending at  $1379 \text{ cm}^{-1}$ ), suggesting a preference for short or mid-sized alkyl chains through these extractions. The above, assisted by the  $\sim 1714 \text{ cm}^{-1}$  acidic carbonyl maxima and  $1415 \text{ cm}^{-1}$  due to C-O-H in-plane bending for #11544, 11550, 11551, 11633, supported the detection of mid- and possibly short-chain FAs in these samples. In other samples, however, such as #11596, only traces of the above were found. Additionally, intense ester carbonyl maxima at  $1738\text{--}1743 \text{ cm}^{-1}$  were detected in most samples from acylglycerols. From the maxima at  $1261 \text{ cm}^{-1}$  ( $\text{CH}_2$  wagging) and  $1182$ , and  $1100 \text{ cm}^{-1}$  (C-O-C antisymmetric stretching of ester links), and  $800 \text{ cm}^{-1}$  (C-O-C bending of ester links) [28,74,75,84], and the low OH stretching intensities ( $\sim 3450 \text{ cm}^{-1}$ ), it can be inferred that diacylglycerols are the predominant esters detected in this solvent.

The above infrared results of the various solvent extracts valuably added to deconstructing the overall profile; for samples #11550 and 11551, this is exemplified in Figure 3d or Figure 4d.

### 3.2. Solvent-Extraction- $\mu$ FTIR

Microscopy-FTIR spectra of selected solvent-extracted samples deposited as films on a gold mirror (abbreviated as SE- $\mu$ FTIR) were recorded in reflection-absorption infrared spectroscopy (RAIRS) mode according to the procedure described in Materials and Methods. This aimed to investigate organic components based on their spatial micro-separation during solvent evaporation on the gold surface [43–45], and therefore, it supported the standard SE-FTIR investigation (see above) by offering more detailed insight into FTIR-detectable components.

SE- $\mu$ FTIR investigations for the sample from oil lamp #11551, after acetone, chloroform, and xylene extractions, gave the most interesting results. The acetone extract of sample #11551 showed the spatial micro-separation and detection of an almost pure medium-chain fatty acid (Figure 4), based on its antisymmetric stretch at  $2928\text{ cm}^{-1}$ .

In the xylene extract, four spots containing fatty acids and various esters (arguably, acylglycerols) in variable amounts on the basis of their carbonyl maxima at  $1746$  (TAG),  $1738$  (DAG),  $1717$  (MAG), and  $1709$  (FA)  $\text{cm}^{-1}$  [74,76,85] were detected in the same deposit, as shown in traces i, ii, ii, and iv of Figure S4. Moreover, the doubly split  $\text{CH}_2$  rocking vibration at  $729$ ,  $720$  of trace i (indicative of the effect of crystalline anisotropy on alkyl chains [74,83,86]), assisted by the downshifted  $2919$ – $2916\text{ cm}^{-1}$  maxima for the antisymmetric  $\text{CH}_2$ , and the acidic carbonyl stretch at  $1709\text{ cm}^{-1}$  [28,64,74,83,87,88] of the xylene extract showed the micro-separation of long-chain fatty acids.

### 3.3. Gas Chromatography–Mass Spectrometry

In all eight samples, a wide range of fatty acids, comprising saturated and mono-unsaturated monocarboxylic acids, as well as oxo-, hydroxyl-, dihydroxy-, and diacids were identified. (Figure 5. Exemplar chromatogram of sample #11551.) Dicarboxylic acids (or diacids) were of both odd and even carbon numbers, ranging from 4 to 15 carbon atoms and in the majority of samples represented the most abundant class of compounds (i.e., samples #11550, 11551, and 11598), with nonanedioic (azelaic) acid predominating. Dihydroxy acids, bearing 18, 20, and 22 carbon atoms (namely, TMS derivatives of 9,10-dihydroxy-octadecanoic acid, 9, 12-dihydroxy-octadecanoic acid, 11,12-dihydroxy-eicosanoic acid, and 13,14-dihydroxy-docosanoic acid, in many cases as pairs of threo-erythro isomers) were also detected in most of the samples, more pronounced in #11550, 11551, and 11633. Fatty acids were primarily of even carbon number (C8 to C26), while odd-numbered members, bearing 9, 15, and 17 carbon atoms, were present in lower abundance and might indicate the addition of animal fat and/or post-depositional contamination (Evershed et al. 1997). The mono-unsaturated C18:1 and C22:1 were found to be present in low abundance and the latter solely in samples #11550 and 11551.

Monoacylglycerols and glycerol were detected, indicating degraded fats/oils. A few samples also appeared to contain traces of the plant sterol  $\beta$ -sitosterol, implying residue of plant origin. In sample #11622A detached from ingot-containing connection areas, low amounts of natural resin-related diterpenic molecules, such as dehydroabietic and 7-oxo-dehydroabietic acid, components of Pinaceae resins in their oxidized state, were detected [89]. As these were found in the connection area of the pedestaled bowl #11622, resin as a flux for soldering purposes was suggested; alternatively, the addition of resins for their aromatic properties was considered, even though they were not detected in any other sample. A synopsis of the compounds identified in all the samples is provided in Figure 6; the chromatograms of all samples and the entire range of identified compounds are presented in detail in Supplementary Data (Figure S2 and Table S1, respectively).

A distinctive feature in the chromatograms was the series of dihydroxy fatty acids (diOH FA) and the relatively polar  $\alpha,\omega$ -dicarboxylic acids detected in all the samples, typically considered as oxidation products of unsaturated fatty acids [8,16,17,90]. Aging tests in Brassicaceae seed oil and investigations of illuminant residues in replica pottery vessels through the burning of various oils [91] explored degradation markers for identifying commodities used as fuel in lamps. The distribution of  $\alpha,\omega$ -dicarboxylic acids, was suggested to directly reflect the position of the double bond in the original product, because vicinal dihydroxy carboxylic acids are formed through dihydroxylation of the double bonds and hence indicate the original position of the double bond in the precursor fatty acids. In particular, it was shown that both 11,12-dihydroxy-eicosanoic (C20diOH) and 13,14-dihydroxy-docosanoic acids (C22diOH) were formed during degradation of 11-eicosenoic (gondoic) and 13-docosenoic acids (erucic), respectively. Similarly, it was suggested that the high proportion of  $\alpha,\omega$ -undecanoic (C11diFA) and  $\alpha,\omega$ -tridecanoic (C13diFA) acids, as well as the presence of shorter chain homologous compounds, were also related to

oxidative mechanisms affecting the higher non-polar unsaturated fatty acids gondoic and erucic [8,16]. The chromatographic profile obtained, comprising degradation products of unsaturated fatty acids, implied the presence of vegetable oils. A typical fatty acid profile, including 15-tetracosenoic (nervonic), 13-docosenoic, 11-eicosenoic and 9-octadecenoic (oleic) acids, as well as their degradation markers is found in members of the Brassicaceae family [8,91,92]. In addition, 9,12-dihydroxyoctadecanoic acid is produced through hydration of 12-hydroxy-octadecenoic acid (ricinoleic acid), found in high abundance in castor oil. Rapeseed and radish oils, products of the same plant family, and castor oil are widely available in the Eastern Mediterranean and have been historically reported as significant sources of natural material with various uses in antiquity [3,6,8,16,91,93,94]. Finally, in the light of FTIR results (see above), the aforementioned detected acidic compounds also included their metal soap counterparts transferred in the worked-up samples, since the BSTFA reagent (see Experimental Procedures) was capable of derivatizing fatty acids and their salts [95].

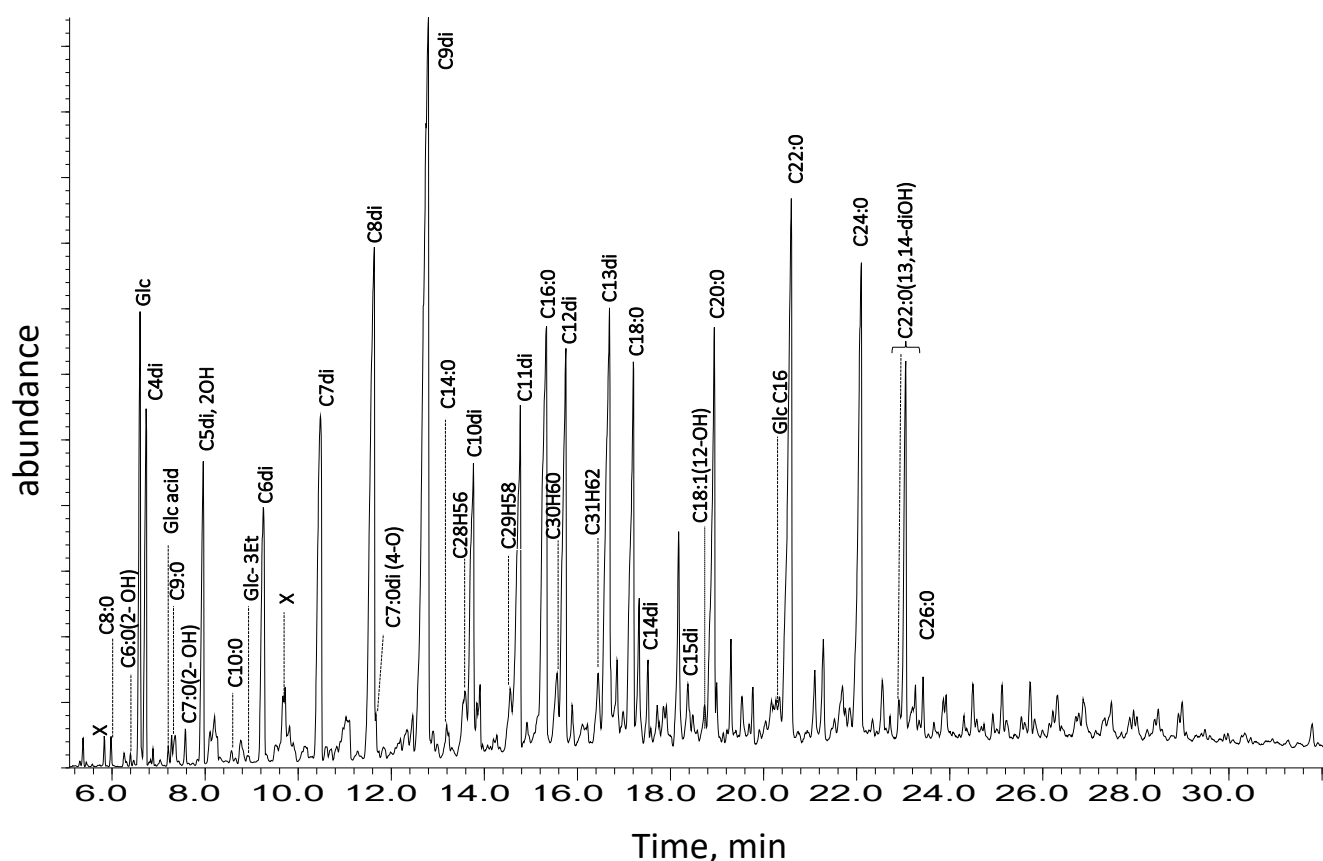


**Figure 5.** Partial total ion chromatogram (TIC) of sample #11551; Key to analyte abbreviations: C8:0 = octanoic acid; C6:0(2-OH) = 2-hydroxy-hexanoic acid; Glc = glycerol; C4di = butanedioic acid; Glc acid = glyceric acid; C9:0 = nonanoic acid; C7:0(2-OH) = 2-hydroxy-heptanoic acid; C5di, 2-OH = 2-hydroxy-glutaric acid; C10:0 = decanoic acid; Glc-3Et = 3-ethyl-glycerol; C6di = hexanedioic acid; C7di = heptanedioic acid; C8di = octanedioic acid; C7di (4-O) = 4-oxo-heptanedioic acid; C9di = nonanedioic acid; C14:0 = tetradecanoic (myristic) acid; C28H56 = octacosene; C10di = decanedioic acid; C29H58 = nonacosene; C11di = undecanedioic acid; C16:0 = hexadecanoic acid (palmitic) acid; C30H60 = triacontene; C12di = dodecanedioic acid; C31H62 = untriacontene; C13di = tridecanedioic acid; C18:0 = octadecanoic (stearic) acid; C14di = tetradecanedioic acid; C15di = pentadecanedioic acid; C18:1(12-OH) = ricinoleic (12-hydroxy-oleic) acid; C20:0 = eicosanoic acid; GlcC16 = palmitoyl-glycerol; C22:0 = docosanoic acid; C24:0 = tetracosanoic acid; C22:0(13,14-diOH) = 13,14-dihydroxy-docosanoic acid; C26:0 = hexacosanoic acid.

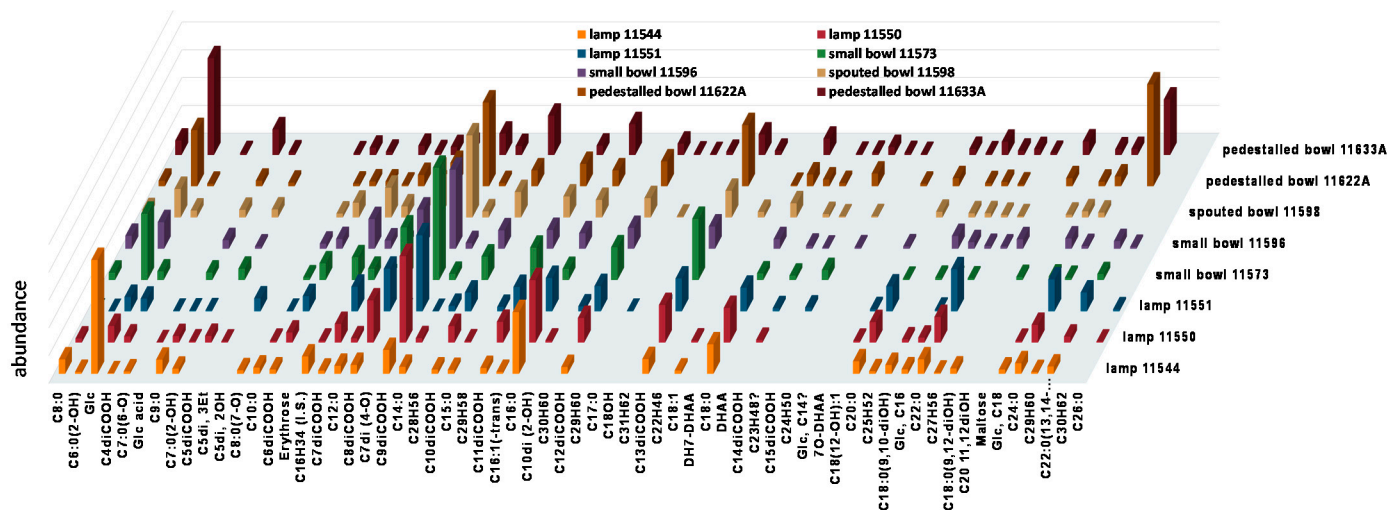


**Figure 6.** Bar graph showing chromatography results of all studied samples. The order of analytes in the horizontal axis is based on their relative retention times in chromatograms, shown in Figures S5a–h. For full names of identified compounds in horizontal axis, consult Table S1.

#### 4. Conclusions

The analysis of visible residues found on the interior surfaces of copper alloy vases from the Benaki Museum Byzantine Collection, dating from the 5th to the 8th centuries AD, provided valuable insights into the potential of residue analysis in non-ceramic material. Organic remains were well preserved, and it was possible to assign the origin of the oil-rich organic materials used/processed in the vessels. In particular, the materials identified in the oil lamps could be related to lighting purposes. On the other hand, the oil residue detected in the small bowls could be related to food processing, cosmetic purposes or other domestic activities.

In the detached samples, the oil material was found in various stages of degradation: esters (possibly of glycerol), fatty acids of long or shorter alkyl chains (indicating fatty substances of both animal and plant origin), and metal salts (soaps), products of possible interaction of the above chemical species with metal cations of the corrosion products or other inorganic remains. The identification of solvent-extractable fatty acid oxidation products (i.e.,  $\alpha,\omega$ -dicarboxylic acids and dihydroxy carboxylic acids, including 9,12-dihydroxyoctadecanoic acid, 11,12-dihydroxy-eicosanoic acid, and 13,14-dihydroxydocosanoic acid), biomarkers and degradation markers of castor oil and Brassicaceae seed oils, allowed the determination of the origin of the residues preserved on the surfaces of the eight metallic vases. Egypt's dry and arid climate offers optimal conditions for the preservation and survival of organic matter [93,95]. The use of cruciferous oil in Egypt has been previously reported in pottery vessels and mollusk shells [91,92,96] and is consistent with ancient sources. However, this is the first time that residues of use in metallic artifacts from Egypt are reported, expanding the range of artifacts [22] that can be studied, providing interpretable results.

After the KBr infrared profile containing numerous inorganic and organic components was broken down by analyzing selected solvent-based organic extracts, compound classes, such as mono-, and di-glycerol esters, free fatty monoacids with various alkyl chain lengths, as well as metal carboxylates, were confirmed. GC-MS provided detailed chemical data and, together with solvent extraction spectra, added significant information to the preliminary FTIR results. This twofold approach facilitated the determination of the specific nature of the residue preserved, providing information on the current condition and the origin of the investigated remains. Another important aspect of this approach addressed the significance of the container remains, with implications for conservation in compliance with widely adopted ethics and for proposing an ultimately informative museological exhibition approach.

**Supplementary Materials:** The following are available online at <https://www.mdpi.com/article/10.3390/heritage4040199/s1>, Figure S1: Infrared spectra of samples extracted from methanol. Intensities of spectra reflect relative quantities of their components; (a) full spectrum, (b) C-H stretching region, and (c) carbonyl stretch and C-H deformation region. Figure S2. Infrared spectra of samples extracted from acetone. Intensities of spectra reflect relative quantities of their components; (a) full spectrum, (b) C-H stretching region, and (c) carbonyl stretch and C-H deformation region. Figure S3. Infrared spectra of samples extracted from dichloromethane. Intensities of spectra reflect relative quantities of their components; (a) full spectrum, and (b) carbonyl stretch and C-H deformation region. Figure S4. Microscopy FTIR spectra of sample #11551 extracted from xylene and deposited on gold mirror disc; spectra (i)–(iv) correspond to four different micro-separated spots on the disc; (a) full spectra; (b) the C-H stretching region, (c) carbonyl region, and (d) methylene rocking region. Figure S5. (a)–(h): Partial total ion gas chromatograms of all samples with main identified components; For a key of abbreviated analytes, see Table S1. IS: Hexadecane (internal standard, see Materials and Methods in main text); x: unknown. Table S1: Organic compounds with relative integration areas detected in the various samples through gas chromatography-mass spectrometry.

**Author Contributions:** K.K.: data curation; investigation; writing—review and editing; S.C.B.: conceptualization; data curation; methodology; project administration; supervision; writing original draft; writing—review and editing; M.R.: data curation; methodology; supervision; writing—review and editing; N.K.: resources; project administration; writing—review and editing; D.K.: conceptualization; project administration; writing—review and editing. All authors have read and agreed to the published version of the manuscript.

**Funding:** Part of this research was pursued in partial fulfillment of Koupadi’s undergraduate thesis; no external funding was received.

**Institutional Review Board Statement:** Not applicable.

**Informed Consent Statement:** Not applicable.

**Acknowledgments:** The authors wish to thank A. Stefanis, Assistant Professor in the Dept. of Conservation of Antiquities and Works of Art, for providing access to digital optical microscopy facilities; Anthea Phoca, Conservator of Antiquities and Works of Art, Benaki Museum, for her involvement in the materials investigations of the Byzantine containers; Anastasia Drandaki, Assistant Professor of Byzantine Archaeology and History of Art, National and Kapodistrian University of Athens, for providing access to the archaeological material. We would also like to thank M. Christea at the Laboratory of Food Chemistry, Biochemistry and Physical Chemistry, Harokopio University, for her valuable help.

**Conflicts of Interest:** The authors declare no conflict of interest.

### Abbreviations

MAG	Mono-fatty Acyl Glycerols
DAG	Di-fatty Acyl Glycerols
TAG	Tri-fatty Acyl Glycerols
DiFA	diacids (dicarboxylic acids)
FA	Fatty Acids
FAMS	Fatty Acids Metal Salts
FTIR	Fourier Transform Infra-Red spectroscopy
GC-MS	gas chromatography–mass spectrometry
SE-FTIR	Solvent-Extracted FTIR
SE- $\mu$ FTIR	Solvent-Extracted microscopy-FTIR

### References

1. Evershed, R.P. Experimental approaches to the interpretation of absorbed organic residues in archaeological ceramics. *World Archaeol.* **2008**, *40*, 26–47. [[CrossRef](#)]
2. Roffet-Salque, M.; Dunne, J.; Alftoft, D.T.; Casanova, E.; Cramp, L.J.; Smyth, J.; Whelton, H.L.; Evershed, R.P. From the inside out: Upscaling organic residue analyses of archaeological ceramics. *J. Archaeol. Sci. Rep.* **2017**, *16*, 627–640. [[CrossRef](#)]
3. Lambert, J.B. Archaeological chemistry. *Acc. Chem. Res.* **2002**, *35*, 583–584. [[CrossRef](#)]

4. Orna, M.V.; Lambert, J.B. New directions in archaeological chemistry. In *Archaeological Chemistry Organic, Inorganic, and Biochemical Analysis*; American Chemical Society: Washington, DC, USA, 1996; pp. 1–9. [[CrossRef](#)]
5. Pollard, A.M.; Batt, C.M.; Stern, B.; Young, S.M.M. *Analytical Chemistry in Archaeology (Cambridge Manuals in Archaeology)*; Cambridge University Press: Cambridge, UK; New York, NY, USA; Melbourne, Australia; Madrid, Spain; Cape Town, South Africa; Singapore; São Paulo, Brazil, 2007.
6. Evershed, R.P. Organic Residue Analysis in Archaeology: The Archaeological Biomarker Revolution. *Archaeometry* **2008**, *50*, 895–924. [[CrossRef](#)]
7. Evershed, R.P. Biomolecular archaeology and lipids. *World Archaeol.* **1993**, *25*, 74–93. [[CrossRef](#)] [[PubMed](#)]
8. Colombini, M.P.; Modugno, F.; Ribechini, E. Organic mass spectrometry in archaeology: Evidence for Brassicaceae seed oil in Egyptian ceramic lamps. *J. Mass Spectrom.* **2005**, *40*, 890–898. [[CrossRef](#)]
9. Pellegrini, D.; Duce, C.; Bonaduce, I.; Biagi, S.; Ghezzi, L.; Colombini, M.P.; Tinè, M.R.; Bramanti, E. Fourier transform infrared spectroscopic study of rabbit glue/inorganic pigments mixtures in fresh and aged reference paint reconstructions. *Microchem. J.* **2016**, *124*, 31–35. [[CrossRef](#)]
10. Degano, I.; La Nasa, J.; Ghelardi, E.; Modugno, F.; Colombini, M.P. Model study of modern oil-based paint media by triacylglycerol profiling in positive and negative ionization modes. *Talanta* **2016**, *161*, 62–70. [[CrossRef](#)]
11. Garnier, N.; Rolando, C.; Høtje, J.M.; Tokarski, C. Analysis of archaeological triacylglycerols by high resolution nanoESI, FT-ICR MS and IRMPD MS/MS: Application to 5th century BC–4th century AD oil lamps from Olbia (Ukraine). *Int. J. Mass Spectrom.* **2009**, *284*, 47–56. [[CrossRef](#)]
12. Gregg, M.W.; Slater, G.F. A new method for extraction, isolation and transesterification of free fatty acids from archaeological pottery. *Archaeometry* **2010**, *52*, 833–854. [[CrossRef](#)]
13. Regert, M.; Garnier, N.; Decavallas, O.; Cren-Oliv, C.C.; Rolando, C. Structural characterization of lipid constituents from natural substances preserved in archaeological environments. *Meas. Sci. Technol.* **2003**, *14*, 1620–1630. [[CrossRef](#)]
14. Ioakimoglou, E.; Boyatzis, S.; Argitis, P.; Fostiridou, A.; Papapanagiotou, K.; Yannovits, N. Thin-Film Study on the Oxidation of Linseed Oil in the Presence of Selected Copper Pigments. *Chem. Mater.* **1999**, *11*, 2013–2022. [[CrossRef](#)]
15. Frankel, E.N. *Lipid Oxidation*, 2nd ed.; Lipid Library Series; Woodhead Publishing/Oily Press: Cambridge, UK, 2005.
16. Colombini, M.P.; Modugno, F. *Organic Mass Spectrometry in Art and Archaeology*, 1st ed.; John Wiley & Sons, Ltd.: Chichester, UK, 2009.
17. Andreotti, A.; Bonaduce, I.; Colombini, M.P.; Gautier, G.; Modugno, A.F.; Ribechini, E. Combined GC/MS analytical procedure for the characterization of glycerolipid, waxy, resinous, and proteinaceous materials in a unique paint microsample. *Anal. Chem.* **2006**, *78*, 4490–4500. [[CrossRef](#)] [[PubMed](#)]
18. Stern, B.; Heron, C.; Tellefsen, T.; Serpico, M. New investigations into the Uluburun resin cargo. *J. Archaeol. Sci.* **2008**, *35*, 2188–2203. [[CrossRef](#)]
19. Stern, B.; Heron, C.; Serpico, M.; Bourriau, J. A comparison of methods for establishing fatty acid concentration gradients across potsherds: A case study using Late Bronze Age Canaanite amphorae. *Archaeometry* **2000**, *42*, 399–414. [[CrossRef](#)]
20. Pitonzo, R.; Armetta, F.; Saladino, M.L.; Oliveri, F.; Tusa, S.; Caponetti, E. Application of Gas Chromatography coupled with Mass Spectrometry (GC/MS) to the analysis of archaeological ceramic amphorae belonging to the Carthaginian fleet that was defeated in the Egadi battle (241 B.C.). *Acta IMEKO* **2017**, *6*, 67–70. [[CrossRef](#)]
21. Blanco-Zubiaguirre, L.; Ribechini, E.; Degano, I.; La Nasa, J.; Carrero, J.A.; Iñáñez, J.; Olivares, M.; Castro, K. GC–MS and HPLC–ESI–QToF characterization of organic lipid residues from ceramic vessels used by Basque whalers from 16th to 17th centuries. *Microchem. J.* **2018**, *137*, 190–203. [[CrossRef](#)]
22. Craig, O.E.; Saul, H.; Spiteri, C. Residue Analysis. In *Archaeological Science*; Richards, M., Britton, K., Eds.; Cambridge University Press: Cambridge, UK, 2019; pp. 70–98.
23. Evershed, R.P.; Berstan, R.; Grew, F.; Copley, M.S.; Charmant, A.J.H.; Barham, E.; Mottram, H.R.; Brown, G. Formulation of a Roman cosmetic. *Nature* **2004**, *432*, 35–36. [[CrossRef](#)] [[PubMed](#)]
24. Frith, J.; Appleby, R.; Stacey, R.; Heron, C. Sweetness and Light: Chemical Evidence of Beeswax and Tallow Candles at Fountains Abbey, North Yorkshire. *Mediev. Archaeol.* **2004**, *48*, 220–227. [[CrossRef](#)]
25. Ribechini, E.; Modugno, F.; Baraldi, C.; Baraldi, P.; Colombini, M.P. An integrated analytical approach for characterizing an organic residue from an archaeological glass bottle recovered in Pompeii (Naples, Italy). *Talanta* **2008**, *74*, 555–561. [[CrossRef](#)]
26. Griffiths, P.R.; Haseth, J.A. *Fourier Transform Infrared Spectrometry*, 2nd ed.; Wiley-Interscience: Hoboken, NJ, USA, 2007.
27. Nakamoto, K. *Infrared and Raman Spectra of Inorganic and Coordination Compounds, Part A: Theory and Applications in Inorganic Chemistry*; Wiley: Hoboken, NJ, USA, 1978.
28. Mayo, D.; Miller, F.; Hannah, R. *Course Notes on the Interpretation of Infrared and Raman Spectra*; John Wiley & Sons, Inc.: Hoboken, NJ, USA, 2004.
29. Derrick, M.R.; Stulik, D.; Landry, J.M. *Infrared Spectroscopy in Conservation Science*; Getty Conservation Institute: Los Angeles, CA, USA, 1999.
30. Stuart, B.H. *Infrared Spectroscopy: Fundamentals and Applications*; John Wiley & Sons, Ltd.: Chichester, UK, 2004.
31. Shillito, L.M.; Almond, M.J.; Wicks, K.; Marshall, L.-J.R.; Matthews, W. The use of FT-IR as a screening technique for organic residue analysis of archaeological samples. *Spectrochim Acta Part A Mol. Biomol. Spectrosc.* **2009**, *72*, 120–125. [[CrossRef](#)] [[PubMed](#)]
32. Thickett, D.; Pretzel, B. FTIR surface analysis for conservation. *Herit. Sci.* **2020**, *8*, 5. [[CrossRef](#)]

33. Bell, J.; Nel, P.; Stuart, B. Non-invasive identification of polymers in cultural heritage collections: Evaluation, optimisation and application of portable FTIR (ATR and external reflectance) spectroscopy to three-dimensional polymer-based objects. *Herit. Sci.* **2019**, *7*, 95. [[CrossRef](#)]
34. Saviello, D.; Toniolo, L.; Goidanich, S.; Casadio, F. Non-invasive identification of plastic materials in museum collections with portable FTIR reflectance spectroscopy: Reference database and practical applications. *Microchem. J.* **2016**, *124*, 868–877. [[CrossRef](#)]
35. Invernizzi, C.; Rovetta, T.; Licchelli, M.; Malagodi, M. Mid and near-infrared reflection spectral database of natural organic materials in the cultural heritage field. *Int. J. Anal. Chem.* **2018**, *2018*, 7823248. [[CrossRef](#)]
36. Tasiouli, N.; Boyatzis, S.; Karatzani, A.; Karydas, A.G. Study and Conservation of a 19th Century Printed Silk Scarf from the Collection of the National Historical Museum of Greece. *Archaeology* **2021**, *9*, 56–67. [[CrossRef](#)]
37. Sommer, A.J. Mid-Infrared Transmission Microspectroscopy. In *Handbook of Vibrational Spectroscopy*; Griffiths, P.R., Ed.; John Wiley & Sons, Ltd.: Chichester, UK, 2006.
38. Pilc, J.; White, R. The Application of FTIR-Microscopy to the Analysis of Paint Binders in Easel Paintings. *Natl. Gallery Tech. Bull.* **1995**, *16*, 73–84.
39. Rizzo, A. Progress in the application of ATR-FTIR microscopy to the study of multi-layered cross-sections from works of art. *Anal. Bioanal. Chem.* **2008**, *392*, 47–55. [[CrossRef](#)]
40. Vetter, W.; Schreiner, M. Characterization of pigment-binding media systems: Comparison of non-invasive in-situ reflection FTIR with transmission FTIR microscopy. *e-Preserv. Sci.* **2011**, *8*, 10–22.
41. Rosi, F.; Legan, L.; Miliiani, C.; Ropret, P. Micro transfection on a metallic stick: An innovative approach of reflection infrared spectroscopy for minimally invasive investigation of painting varnishes. *Anal. Bioanal. Chem.* **2017**, *409*, 3187–3197. [[CrossRef](#)]
42. Ajò, D.; Casellato, U.; Fiorin, E.; Vigato, P. Ciro Ferri's frescoes: A study of painting materials and technique by SEM-EDS microscopy, X-ray diffraction, micro FT-IR and photoluminescence spectroscopy. *J. Cult. Herit.* **2004**, *5*, 333–348. [[CrossRef](#)]
43. Sciutto, G.; Oliveri, P.; Prati, S.; Catelli, E.; Bonacini, I.; Mazzeo, R. A Multivariate Methodological Workflow for the Analysis of FTIR Chemical Mapping Applied on Historic Paint Stratigraphies. *Int. J. Anal. Chem.* **2017**, *2017*, 4938145. [[CrossRef](#)] [[PubMed](#)]
44. La Russa, M.F.; Ruffolo, S.A.; Crisci, G.M.; Barone, G.; Mazzoleni, P.; Pezzino, A. The Use of FTIR and Micro-FTIR Spectroscopy: An Example of Application to Cultural Heritage. *Int. J. Spectrosc.* **2009**, *2009*, 893528. [[CrossRef](#)]
45. Kotzamani, D.; Phoca, A.; Karydi, G.; Zacharia, M.; Kantarelou, V.; Karatasios, J.; Boyatzis, S.C.; Perdikatsis, V. The Metallurgical Investigation of Copper-Alloys Metalwork of The Benaki Museum Dated in the 4–7th Centuries A.D. In Proceedings of the International Symposium on History, Technology and Conservation of Ancient Metal, Glasses and Enamels, Athens, Greece, 16–19 November 2011.
46. Boyatzis, S.C.; Kotzamani, D.; Phoca, A.; Karydi, G.; Zacharia, M.; Kantarelou, V. Characterization of organic remains found in copper alloy vessels of the Benaki museum collection with Fourier-transform infrared spectroscopy. In Proceedings of the 3rd ARCH\_RNT, Archaeological Research and New Technologies, Kalamata, Greece, 3–5 October 2012; Zacharias, N., Ed.; University of the Peloponnese: Tripoli, Greece, 2014; pp. 95–102.
47. Drandaki, A. *Late Antique Metalware, Bibliothèque de L'Antiquité, Tardive*; Brepole Publishers: Turnhout, Belgium, 2020.
48. Arya, R.K. Drying induced phase separation in multicomponent polymeric coatings—Simulation study. *Int. J. Sci. Technol. Res.* **2012**, *1*, 48–52.
49. Mitchell, D.S. *Solvent Extraction Process*; OSTI: Oak Ridge, TN, USA, 1980.
50. THolcombe, T.C.; Bress, D.F.; Casparian, R.E. Process for Drying and Solvent-Extraction of Solids and Sludges. International Patent WO1992022367A1, 23 December 1992.
51. Orata, F. Derivatization reactions and reagents for gas chromatography analysis. In *Advanced Gas Chromatography—Progress in Agricultural, Biomedical and Industrial Applications*; InTech: Rijeka, Croatia, 2012; pp. 83–156. [[CrossRef](#)]
52. Husek, P. Derivatization. In *Encyclopedia of Separation Science*; Academic Press: Cambridge, MA, USA, 2000; pp. 434–443.
53. Colombini, M.P.; Modugno, F.; Giacomelli, M.; Francesconi, S. Characterisation of proteinaceous binders and drying oils in wall painting samples by gas chromatography-mass spectrometry. *J. Chromatogr. A* **1999**, *846*, 113–124. [[CrossRef](#)]
54. Weiner, S. *Microarchaeology*, 1st ed.; Cambridge University Press: Cambridge, UK, 2010.
55. Nevin, A.; Melia, J.L.; Osticioli, I.; Gautier, G.; Colombini, M.P. The identification of copper oxalates in a 16th century Cypriot exterior wall painting using micro FTIR, micro Raman spectroscopy and Gas Chromatography-Mass Spectrometry. *J. Cult. Herit.* **2008**, *9*, 154–161. [[CrossRef](#)]
56. Purvis, O.W. The Occurrence of Copper Oxalate in Lichens Growing on Copper Sulphide-Bearing Rocks in Scandinavia. *Lichenologist* **1984**, *16*, 197–204. [[CrossRef](#)]
57. Bellamy, L.J. *The Infra-Red Spectra of Complex Molecules*; Springer: Dordrecht, The Netherlands, 1975.
58. Larkin, P. *Infrared and Raman Spectroscopy: Principles and Spectral Interpretation*; Elsevier: Amsterdam, The Netherlands, 2011.
59. Coates, J. Interpretation of Infrared Spectra, A Practical Approach. In *Encyclopedia of Analytical Chemistry*; John Wiley & Sons, Ltd.: Chichester, UK, 2006; pp. 10815–10837.
60. Lambert, J.B.; Shurvell, H.F.; Cooks, R.G. *Introduction to Organic Spectroscopy*, 1st ed.; Macmillan: New York, NY, USA, 1987.
61. Nakamoto, K. *Infrared and Raman Spectra of Inorganic and Coordination Compounds, Part B, Applications in Coordination, Organometallic, and Bioinorganic Chemistry*, 6th ed.; John Wiley & Sons: Hoboken, NJ, USA, 2009.

62. Baeten, J.; Romanus, K.; Degryse, P.; De Clercq, W.; Poelman, H.; Verbeke, K.; Luypaerts, A.; Walton, M.; Jacobs, P.; De Vos, D.; et al. Application of a multi-analytical toolset to a 16th century ointment: Identification as lead plaster mixed with beeswax. *Microchem. J.* **2010**, *95*, 227–234. [[CrossRef](#)]
63. Hammann, S.; Scurr, D.J.; Alexander, M.R.; Cramp, L.J.E. Mechanisms of lipid preservation in archaeological clay ceramics revealed by mass spectrometry imaging. *Proc. Natl. Acad. Sci. USA* **2020**, *117*, 14688–14693. [[CrossRef](#)]
64. Anna Filopoulou Vlachou, S.; Boyatzis, S.C. Fatty Acids and Their Metal Salts: A Review of Their Infrared Spectra in Light of Their Presence in Cultural Heritage (accepted for publication). *Molecules* **2021**, in press.
65. Lynch, M.L.; Pan, A.Y.; Laughlin, R.G. Spectroscopic and Thermal Characterization of 1:2 Sodium Soap/Fatty Acid Acid—Soap Crystals. *J. Phys. Chem.* **1996**, *100*, 357–361. [[CrossRef](#)]
66. Otero, V.; Sanches, D.; Montagner, C.; Vilarigues, M.; Carlyle, L.; Lopes, J.A.; Melo, M.J. Characterisation of metal carboxylates by Raman and infrared spectroscopy in works of art. *J. Raman Spectrosc.* **2014**, *45*, 1197–1206. [[CrossRef](#)]
67. Baij, L.; Hermans, J.J.; Keune, K.; Iedema, P. Time-Dependent ATR-FTIR Spectroscopic Studies on Fatty Acid Diffusion and the Formation of Metal Soaps in Oil Paint Model Systems. *Angew. Chem. Int. Ed.* **2018**, *57*, 7351–7354. [[CrossRef](#)] [[PubMed](#)]
68. Kazarian, S.; Chan, K. Applications of ATR-FTIR spectroscopic imaging to biomedical samples. *Biochim. Biophys. Acta Biomembr.* **2006**, *1758*, 858–867. [[CrossRef](#)] [[PubMed](#)]
69. Hermans, J.J. *Metal Soaps in Oil Paint: Structure, Mechanisms and Dynamics*; University of Amsterdam: Amsterdam, The Netherlands, 2017.
70. Catalano, J.; Yao, Y.; Murphy, A.; Zumbulyadis, N.; Centeno, S.A.; Dybowski, C. Analysis of Lead Carboxylates and Lead-Containing Pigments in Oil Paintings by Solid-State Nuclear Magnetic Resonance. *MRS Proc.* **2014**, *1656*, 149–156. [[CrossRef](#)]
71. Hermans, J.J.; Keune, K.; van Loon, A.; Iedema, P.D. The crystallization of metal soaps and fatty acids in oil paint model systems. *Phys. Chem. Chem. Phys.* **2016**, *18*, 10896–10905. [[CrossRef](#)] [[PubMed](#)]
72. McGovern, P.E.; Hall, G.R. Charting a Future Course for Organic Residue Analysis in Archaeology. *J. Archaeol. Method Theory* **2015**, *23*, 592–622. [[CrossRef](#)]
73. Chapman, D. Infrared spectroscopy of lipids. *J. Am. Oil Chem. Soc.* **1965**, *42*, 353–371. [[CrossRef](#)]
74. Jackson, M.; Haris, P.I.; Chapman, D. Fourier transform infrared spectroscopic studies of lipids, polypeptides and proteins. *J. Mol. Struct.* **1989**, *214*, 329–355. [[CrossRef](#)]
75. Chapman, D. Infrared spectra and the polymorphism of glycerides. Part II. 1:3-Diglycerides and saturated triglycerides. *J. Chem. Soc.* **1956**, 2522–2528. [[CrossRef](#)]
76. Boyatzis, S.C.; Douvas, A.M.; Argyropoulos, V.; Siatou, A.; Vlachopoulou, M. Characterization of a water-dispersible metal protective coating with fourier transform infrared spectroscopy, modulated differential scanning calorimetry, and ellipsometry. *Appl. Spectrosc.* **2012**, *66*, 580–590. [[CrossRef](#)]
77. Jones, R.N. The Effects of Chain Length on the Infrared Spectra of Fatty Acids and Methyl Esters. *Can. J. Chem.* **1962**, *40*, 321–333. [[CrossRef](#)]
78. Meiklejohn, R.A.; Meyer, R.J.; Aronovic, S.M.; Schuette, H.A.; Meloche, V.W. Characterization of Long-Chain Fatty Acids by Infrared Spectroscopy. *Anal. Chem.* **1957**, *29*, 329–334. [[CrossRef](#)]
79. De Ruig, W.G. *Infrared Spectra of Monoacid Triglycerides with Some Applications to Fat Analysis*; Center for Agricultural Publishing and Documentation: Wageningen, The Netherlands, 1971.
80. Tiwari, R.D.; Sharma, J.P.; Belcher, R. *The Determination of Carboxylic Functional Groups: Monographs in Organic Chemistry*; Elsevier: Amsterdam, The Netherlands, 2013.
81. Frankel, E.N. Lipid oxidation: Mechanisms, products and biological significance. *J. Am. Oil Chem. Soc.* **1984**, *61*, 1908–1917. [[CrossRef](#)]
82. Corish, P.J.; Chapman, D. The infrared spectra of some monocarboxylic acids. *J. Chem. Soc.* **1957**, *18*, 1746–1751. [[CrossRef](#)]
83. O'Connor, R.T.; DuPre, E.F.; Feuge, R.O. The infrared spectra of mono-, di-, and triglycerides. *J. Am. Oil Chem. Soc.* **1955**, *32*, 88–93. [[CrossRef](#)]
84. Chapman, D. The Polymorphism of Glycerides. *Chem. Rev.* **1962**, *62*, 433–456. [[CrossRef](#)]
85. Chapman, D. The 720 cm<sup>-1</sup> band in the infrared spectra of crystalline long-chain compounds. *J. Chem. Soc.* **1957**, *18*, 4489–4491. [[CrossRef](#)]
86. Shurvell, H.F. Spectra-Structure Correlations in the Mid- and Far-Infrared. In *Handbook of Vibrational Spectroscopy*; Chalmers, J.M., Ed.; John Wiley & Sons, Ltd.: Chichester, UK, 2006.
87. Lewis, R.N.A.H.; McElhaney, R.N. Vibrational Spectroscopy of Lipids. In *Handbook of Vibrational Spectroscopy*; Griffiths, P.R., Ed.; John Wiley & Sons, Ltd.: Chichester, UK, 2006.
88. Regert, M. Investigating the history of prehistoric glues by gas chromatography—Mass spectrometry Original Paper. *J. Sep. Sci.* **2004**, *27*, 244–254. [[CrossRef](#)]
89. Boyatzis, S.; Ioakimoglou, E.; Argitis, P. UV exposure and temperature effects on curing mechanisms in thin linseed oil films: Spectroscopic and chromatographic studies. *J. Appl. Polym. Sci.* **2002**, *84*, 936–949. [[CrossRef](#)]
90. Copley, M.S.; Bland, H.A.; Rose, P.; Horton, M.; Evershed, R.P. Gas chromatographic, mass spectrometric and stable carbon isotopic investigations of organic residues of plant oils and animal fats employed as illuminants in archaeological lamps from Egypt. *Analyst* **2005**, *130*, 860–871. [[CrossRef](#)]

91. Romanus, K.; Van Neer, W.; Marinova, E.; Verbeke, K.; Luypaerts, A.; Accardo, S.; Hermans, I.; Jacobs, P.; De Vos, D.; Waelkens, M. Brassicaceae seed oil identified as illuminant in Nilotic shells from a first millennium AD Coptic church in Bawit, Egypt. *Anal. Bioanal. Chem.* **2007**, *390*, 783–793. [[CrossRef](#)] [[PubMed](#)]
92. Lucas, A.; Harris, J.R. *Ancient Egyptian Materials and Industries*; Histories and Mysteries of Man, Ltd.: London, UK, 1962.
93. Serpico, M.; White, R. Oil, fat and wax. In *Ancient Egyptian Materials and Technology*; Nicholson, P.T., Shaw, I., Eds.; Cambridge University Press: Cambridge, UK, 2000; pp. 390–429.
94. La Nasa, J.; Modugno, F.; Aloisi, M.; Lluveras-Tenorio, A.; Bonaduce, I. Development of a GC/MS method for the qualitative and quantitative analysis of mixtures of free fatty acids and metal soaps in paint samples. *Anal. Chim. Acta* **2018**, *1001*, 51–58. [[CrossRef](#)] [[PubMed](#)]
95. Regert, M.; Bland, H.A.; Dudd, S.N.; Van Bergen, P.F.; Evershed, R.P. Free and bound fatty acid oxidation products in archaeological ceramic vessels. *Proc. R. Soc. B Boil. Sci.* **1998**, *265*, 2027–2032. [[CrossRef](#)]
96. Colombini, M.P.; Modugno, F.; Ribechini, E. Direct exposure electron ionization mass spectrometry and gas chromatography/mass spectrometry techniques to study organic coatings on archaeological amphorae. *J. Mass Spectrom.* **2005**, *40*, 675–687. [[CrossRef](#)] [[PubMed](#)]